

# Serial sectioning and three-dimensional reconstruction of mouse Peyer's patch

Bin Ma<sup>a,\*</sup>, Lei Wang<sup>a</sup>, Reinhard von Wasielewski<sup>b</sup>,  
Werner Lindenmaier<sup>a</sup>, Kurt E.J. Dittmar<sup>a,\*</sup>

<sup>a</sup>Gene Regulation and Differentiation, Helmholtz Centre for Infection Research, Inhoffenstrasse 7, D-38124 Braunschweig, Germany

<sup>b</sup>Histo-Pathology Unit, Helmholtz Centre for Infection Research, Braunschweig, Germany

Received 12 August 2007; received in revised form 15 October 2007; accepted 15 October 2007

## Abstract

Peyer's patches (PPs) are typical gut-associated lymphoid tissues that are located along the wall of the small intestine and that serve as the major sites for generation of immunity to intestinal antigens. Their unique micro-organization is crucial for the generation of the immune response. Although many studies have been reported on the functional anatomy of PP, most investigations have relied on the random sampling of these organs, a procedure that is insufficient for the systemic scanning of the whole tissue or organ. By combining a variety of methods, we have accomplished 3D reconstructions of Peyer's patch. The complex reconstruction procedure includes several steps. First, the PP are serially sectioned at a thickness of 10  $\mu\text{m}$  with a cryostat; (b) the serial sections are stained with haematoxylin–eosin; (c) multiple images from the PP are acquired with an automatic microscope and stitched together with Image Pro Plus to generate a composite image for the whole organ; (d) the serial images are reconstructed with Image J, Reconstruct and 3D Studio Max. The combinational approaches that we present here should be of value when extrapolated to the reconstruction of other tissues or organs. Moreover, the 3D model that we have created and our stereological analysis should be extremely helpful for further *in vivo* microscopic studies of PP with respect to the immune response.

© 2007 Elsevier Ltd. All rights reserved.

**Keywords:** Serial section; 3D reconstruction; Mouse; Peyer's patch

## 1. Introduction

Although the gastrointestinal mucosa is indispensable for its absorptive functions, it also represents the port of entry for many pathogens. It is responsible for keeping invading pathogens out and protecting the host from infection through an integrated network of tissues, lymphoid cells, constitutive cells and effectors molecules (Steinman and Witmer, 1984; Young et al., 2003; Brandtzaeg and Pabst, 2004). Gut and gut-associated lymphoid tissues (GALT) can be regarded as the largest secondary lymphoid organs. Peyer's patches (PPs) are typical GALTs that are located along the wall of the small intestine and that serve as the major sites for the generation of immunity to intestinal antigens. Their unique micro-organization is crucial for the generation of the immune response. For

example, specialized epithelial cells, called M cells, located in the follicle-associated epithelium (FAE) of the PP and the dendritic cells beneath the subepithelial dome (SED), can sample antigens from the intestine lumen (Kelsall and Strober, 1996; Sato and Iwasaki, 2005; Iwasaki, 2007). Lymphocytes enter the PP through a postcapillary high endothelial venule by homing mechanisms and stimulated lymphocytes to exit from the PP through the efferent lymphatic vessels (Okada et al., 2002; Warnock et al., 2000).

Many studies have been reported on the functional anatomy of PP (Ermak and Owen, 1986; Brandtzaeg and Pabst, 2004; Ma et al., 2007a). However, most studies have relied on the random sampling of these organs. Therefore, systemic scans of the whole tissue or organ should now ideally be made. Three-dimensional (3D) reconstructions can conveniently be used to visualize a statistically significant number of individual structures, while retaining their localization with respect to each other in the organ. In addition, 3D data is a prerequisite for *in vivo* microscopic studies of organs such as the PP (Kunkel et al., 1998; Bargatze et al., 1995; Wagner et al., 1996).

\* Corresponding authors. Tel.: +49 531 6181 5017; fax: +49 531 6181 5012.

E-mail addresses: [bin.ma@yale.edu](mailto:bin.ma@yale.edu) (B. Ma), [ked@helmholtz-hzi.de](mailto:ked@helmholtz-hzi.de) (K.E.J. Dittmar).

To perform the 3D reconstruction of a whole organ, several challenges have to be overcome. First, the whole organ must be properly serially sectioned and stained. Both paraffin sections and resin sections can be used for 3D reconstructions (Steiniger et al., 2003; Fujimura and Nozaka, 2002; Süß et al., 2002). Various staining methods, such as toluidine blue, haematoxylin–eosin (HE) and immunohistochemistry, have been applied for the histological analysis and segmentation of the sectioned structures or objects (Süß et al., 2002; Fujimura and Nozaka, 2002; Steiniger et al., 2003). In our study, a combinational approach of serial cryosectioning and haematoxylin–eosin staining has been applied. Second, the section series must be digitized and properly aligned for further 3D reconstruction steps. Since, during the digitization of the sections, single acquisition is impossible in most cases with regard to taking a whole image from the complete organ at high resolution, multiple images from parts of each section must be acquired and stitched or tiled together manually or automatically with various programs (Ma et al., 2007b; Süß et al., 2002). In addition, the orientation of each of the sections is different because of the manual mounting of sections on the slides. In order to align these serial sections, both manual and automatic approaches have been applied (Fujimura and Nozaka, 2002; Ma et al., *in press*). Third, a 3D reconstruction program has to be chosen and applied for the 3D reconstruction. Many programs such as AutoCAD, 3D Doctor and warp filtering can be used for 3D reconstructions and further stereological analysis (Süß et al., 2002; Steiniger et al., 2003; Ju et al., 2006). In our study, we have applied a free program, named Reconstruct, for our 3D reconstruction of the PP following the preparation of serial sections.

## 2. Material and methods

### 2.1. Mice

BALB/c female mice (8–12 weeks old) were obtained from Harlan Winkelmann (Borchen, Germany). They were maintained under specific pathogen-free conditions in the animal facility of the Helmholtz Centre for Infection Research.

### 2.2. Section preparation

Mice were killed by CO<sub>2</sub> narcosis and the ileum (including Peyer's patch) from each mouse was quickly removed, embedded in Tissue-Tek<sup>®</sup> OCT (optimal cutting temperature) Compound (Sakura Finetek, Torrance, CA, USA) and snap-frozen in liquid nitrogen. 10 µm serial cryosections were prepared with a Reichert-Jung 2800e Cryostat (Leica, Wetzlar, Germany). The cutting direction is vertical to the long axis of the ileum. In total, four pieces of ileum were sectioned and one representative serial section set was presented. This serial section set included 226 sections.

### 2.3. Haematoxylin–eosin staining

Cryosections were mounted on self-prepared poly-lysine-coated slides, air-dried for 10 min and fixed in 10% neutral

buffered formaldehyde (Carl Roth, Karlsruhe, Germany) for 10 min. After being washed with running tap water for 3 min, the sections were stained with Mayer's Haemalaun (Merck, Darmstadt, Germany) for 10 min. Following differentiation in freshly prepared 3.75% HCl (in 70% ethanol), the sections were washed with running tap water for another 5 min, dehydrated in 70% and 90% ethanol for 2 min each, stained with alcoholic eosin (containing 0.1% phloxine in 90% ethanol; Sigma–Aldrich, Steinheim, Germany) for 5 min, dehydrated in 100% ethanol and xylene and finally mounted in Entellan New (Merck, Darmstadt, Germany) mounting medium.

### 2.4. Image acquisition

An Olympus 1 × 71 inverted microscope (OLYMPUS, Hamburg, Germany), equipped with a Märzhäuser automated slide-positioning stage (Scan IM 100 × 100, Märzhäuser, Germany) operated through an OASIS-4i PCI controller (Objective Imaging, Cambridge, UK) and a QICam CCD Colour Camera (QImaging, Burnaby, BC, Canada), was used for the automatic acquisition of images. The repetition accuracy of the positioning stage was ±0.50 µm. The images were taken via a 20× 0.75 NA objective lens. The program Surveyor (Version 3.0, Objective Imaging, Cambridge, UK) was used in the standard-scan mode for image acquisition. The complete system was set up by CHROMAPHOR Analysen-Technik GmbH (Ascheberg, Germany). An IBM Intellistation workstation (Pentium IV processor; CPU: 3.20 GHz; RAM: 3.5 G) with Microsoft Windows XP (Professional edition) as the operation system was employed.

For a single section, 24 small images (4 × 6) were acquired at a resolution of 1388 × 1036 pixels (size: 4.11 MB). These images were stored in the format of a BMP file stack.

For further image processing and 3D reconstruction, a Dell Optiplex GX620 PC (Pentium IV processor) was used (CPU: 3.20 GHz; RAM: 3.5 G) with Microsoft Windows XP (Professional edition) as the operation system.

### 2.5. Image stitching

Image-Pro Plus (Version 5.1) was obtained from Media Cybernetics (Silver Spring, MD, USA). The image stack containing 24 small images was imported into the program and the “Tiling” function in the menu “Process” was used for stitching as follows: tiling method: Fourier correlation; correlation mode: phase correlation; stitching method: gradient blend; always recalculate: selected; original size after stitching: 5096 × 5216 pixels (76.0 MB).

### 2.6. Image processing

After stitching, the lymphoid tissue part (Peyer's patch) was segmented from the composite image and copied to a template (2400 × 2400, 16.5 MB) to a new serial image data set. The size and brightness/contrast of these images were then adjusted by Paint Shop Pro 9 (Jasc Software, Inc., Minneapolis, MN, USA).

## 2.7. Image registration

The free program Reconstruct (Version 1.0.7.0) was downloaded from the website <http://synapses.bu.edu/tools/download.htm>. Rigid transformations including translation and rotation were performed manually via the keyboard to align two adjacent images. No scaling or perspective was used for the registration. After registration, the images were exported as a stack of images, which were then cropped and re-sized for further 3D reconstructions.

To test the performance of registration, adjacent images were overlaid by the Paint Shop Pro 9. The transparencies of the second images were set to 50% for visualization of the match of the two adjacent sections. The combined image was then exported to generate one single image for a comparison of the two sections.

## 2.8. 3D reconstruction

Cinepak Codec by Radius was used for the compression of video files.

### 2.8.1. 3D reconstruction with Image J

Image J (Version 1.37v) was from National Institutes of Health (<http://rsb.info.nih.gov/ij/>). The maximum memory used was 1200 MB. Movies were compressed with Virtual Dub (Version 1.6.17, [www.virtualdub.org](http://www.virtualdub.org)).

- The image stack containing 226 serial sections was imported into Image J. Of these, 34 were selected and tiled together by using “make montage” in the menu “Stack”. The whole image stack was saved as uncompressed AVI files and then compressed to generate normal AVI documents.
- After inversion of the whole image stack by using “Invert” in the Edit menu, 3D reconstructions were performed by means of “3D project”. The settings for the 3D projection were: rotation angle increment: 10; opacity: 0; surface depth-cueing: 50%; interior depth-cueing: 50%; projection methods: brightest point; axis of rotation: Y-axis; slice spacing: 2.13 pixels; interpolate: selected. After projection, the whole stack of 36 images (projections) was inverted once again to generate the normal 3D projections.

### 2.8.2. 3D reconstruction with Reconstruct

Germinal centres, follicles and the whole Peyer’s patch were manually traced from the image serials and mapped with yellow, blue and magenta, respectively. The morphology of these compartments and the correlation of the same structures in the adjacent sections were considered for the tracing of these compartments on serial images. For 3D views, Boissonnat surfaces were generated by using the compartments’ traces taken from the sections. The colour and transparency of the objects were then adjusted for better visualization. The rendering results were exported as BMP files. In all, 13 serial images (angle increment: 30°) were generated manually and imported to Image J to generate the 3D projection video.

### 2.8.3. 3D reconstruction with 3D Studio MAX

3D Studio MAX (Version 7.0) was obtained from Autodesk (San Rafael, CA, USA). In Reconstruct, sets of objects were imported to the 3D view and exported as VRML files (Boissonnat surface model). These VRML files were then

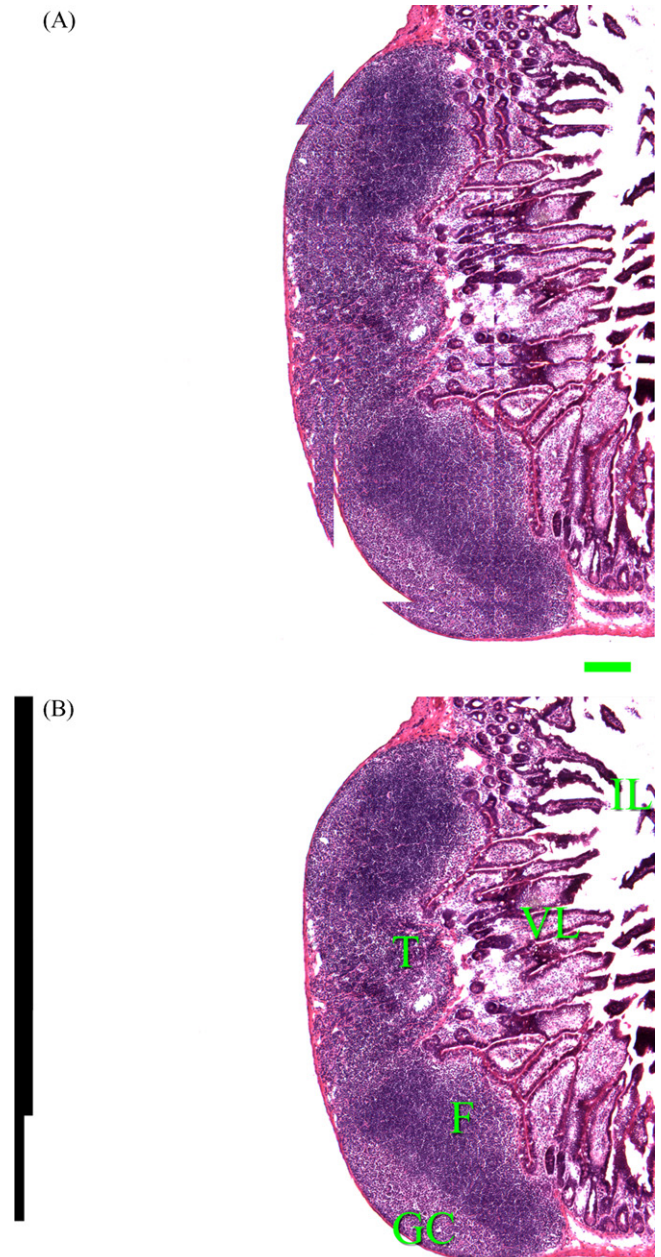


Fig. 1. Single image of a whole mouse Peyer’s patch generated by the stitching of 24 images acquired by the automatic microscope. The sizes of the images were optimized. Slice number in the serial section set: 119; IL: intestine lumen; VL: villus; T: T cell dependent region; F: follicle; GC: germinal centre. (A) 24 small images (4 × 6), each of which has 12% overlap with the adjacent image, were tiled with Image J. Objective lens: 20×; original small images format: stack of BMP files; single small image size: 1388 × 1036 (4.11 MB); bar: 200 μm. (B) The stitched results generated by Image-Pro Plus. Tiling method: Fourier correlation; correlation mode: phase correlation; stitching method: gradient blend; always recalculate: selected; original size of composite image after stitching: 5096 × 5216 (76.0 M); reduced size: 1388 × 1421 (300 dpi); format: TIFF.

imported to 3D Studio Max for smoothing and rendering. The follicle object set, germinal centre object set and the whole Peyer's patch were imported separately as three VRML files.

Relax modifier was applied for first step of smoothing: repeat times: 8. Mesh smoother was then used for the further smoothing step. All the smoothing groups were selected: repeat times: 4. After smoothing, the colour and transparency of objects were adjusted for better visualization. Finally, the rendering results (3D presentation) were imported as BMP files.

### 3. Results

In total, 226 serial sections ( $10\ \mu\text{m}$ ) from a mouse ileum were prepared with a cryostat and stained with haematoxylin–eosin. To acquire images for the Peyer's patch at high resolution ( $200\times$ ), multiple small images ( $4 \times 6$ , with 12% overlap with

adjacent image) from the Peyer's patch were acquired and stitched with Image Pro Plus. The results are shown in Fig. 1.

Manual registration function was applied for the registration of the serial sections. In Fig. 2, this step of registration is demonstrated for eight serial sections from the data set. The performance of the registration was tested by blending two adjacent sections (Supplementary Fig. 1). Parts of the aligned image series are shown in Fig. 3. Animation of this whole series is shown in Supplementary video 1.

Three methods were applied for the 3D reconstruction of the Peyer's patch. First, Image J was applied for the 3D reconstruction of Peyer's patch. The reconstruction results are shown in Fig. 4 and Supplementary video 2 and 3. Second, with Reconstruct, various compartments of Peyer's patch were manually traced and used for the reconstruction. The results are shown in Fig. 5 and Supplementary video 4. In the PP studied,

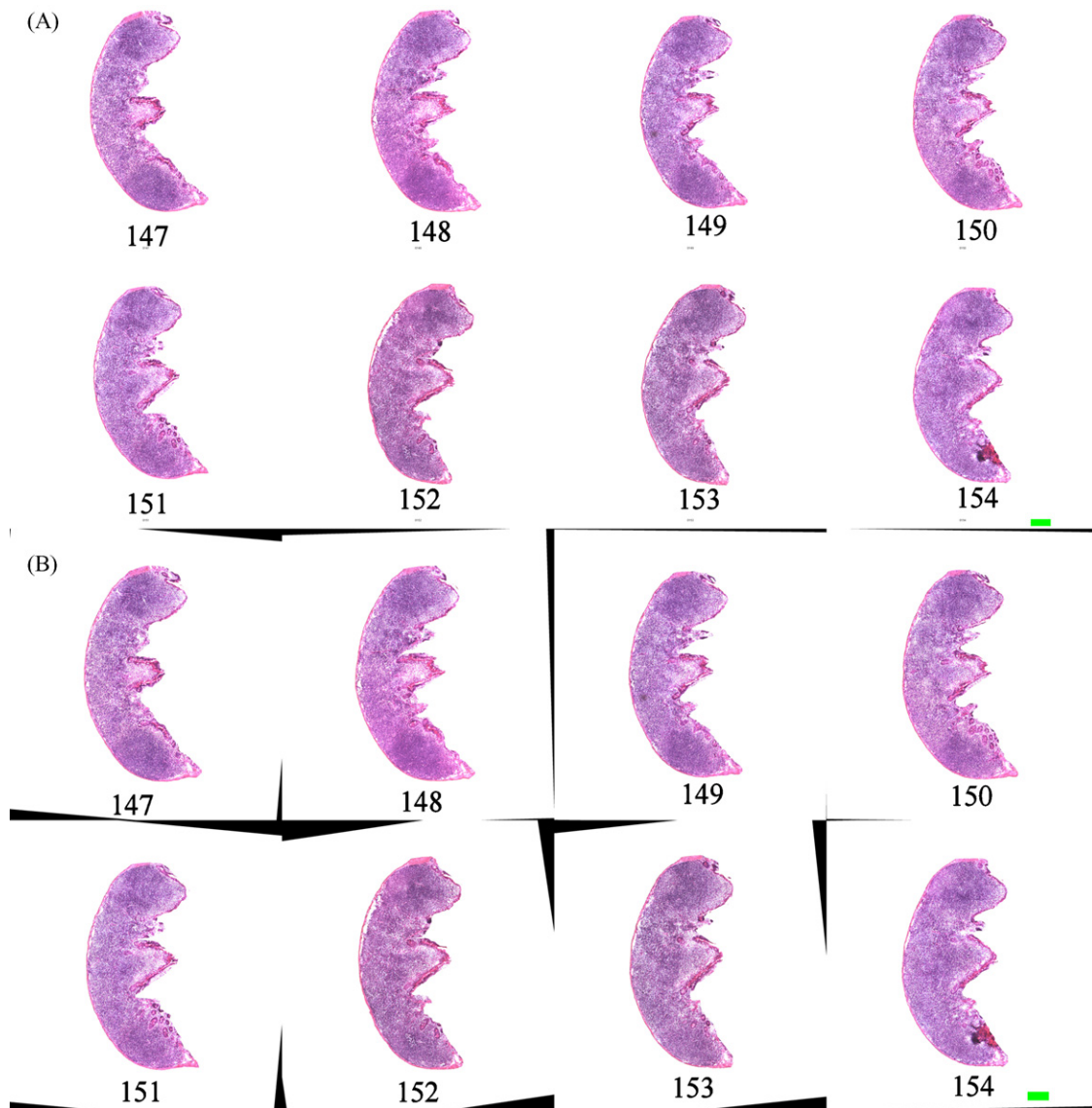


Fig. 2. Alignment of serial sections from the mouse Peyer's patch by using Reconstruct. The sizes of the images were optimized. The section number is indicated under the images. Bar:  $200\ \mu\text{m}$ . (A) Eight serial sections (from no. 147 to no. 154) before alignment. Only the lymphoid portion of the small intestine was segmented from the images. (B) Eight serial sections after alignment. Registration method: manual registration. Please note that the images were cropped from the composite image to remove black or white background information.

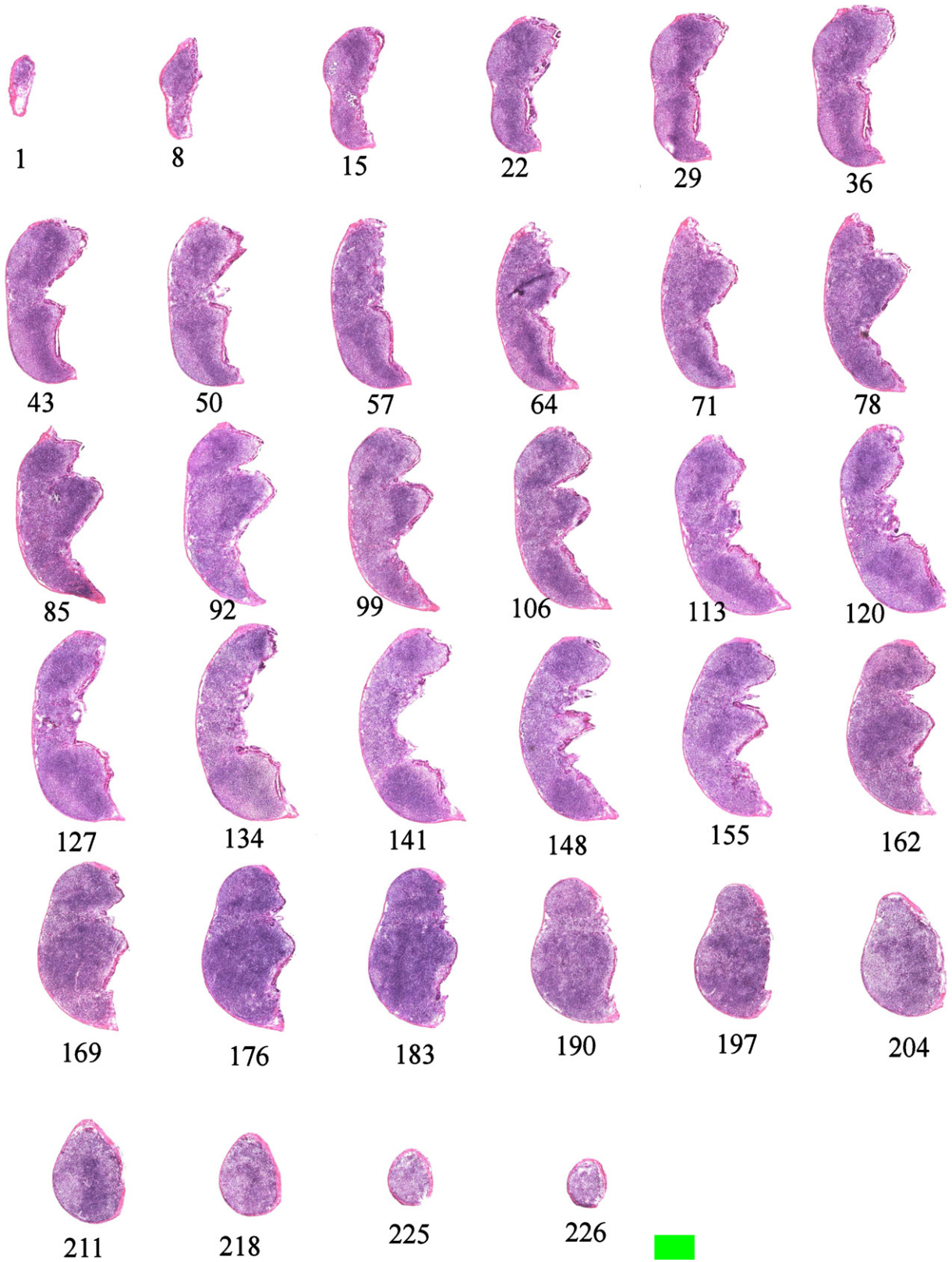


Fig. 3. 34 sections from the serial section dataset (226 sections in total). The sizes of the images were optimized. The number of the sections is indicated under the images. Bar: 1000  $\mu\text{m}$ .

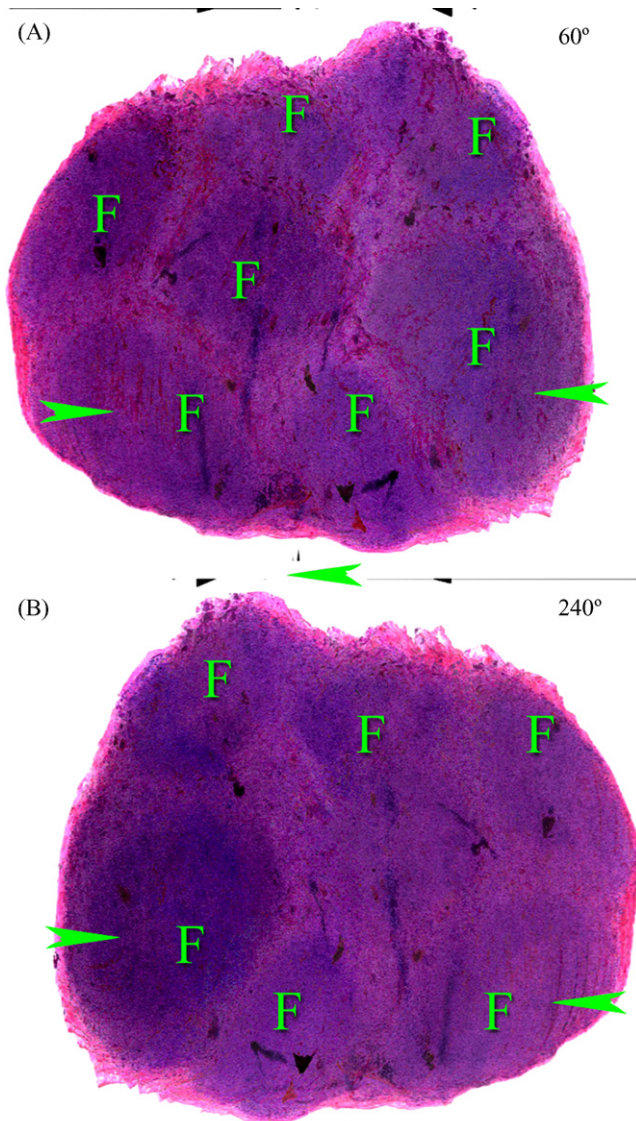


Fig. 4. 3D reconstruction of a mouse Peyer's patch by using Image J. Two projections from the reconstructions results are shown. The brightness/contrast and size of the images were optimized after reconstruction. The settings for the 3D projection were: rotation angle increment: 10; opacity: 0; surface depth-cueing: 50%; interior depth-cueing: 50%; projection methods: brightest point; axis of rotation: Y-axis; slice spacing: 2.13 pixels; interpolate: selected. F: follicle. The positions of germinal centres are indicated by arrows. (A) Rotation angle: 60° (forward). (B) Rotation angle: 240° (backward).

there were eight follicles and seven of them had germinal centres. The relative volume of the germinal centres and follicles are shown in [Supplementary Table 1](#). Third, to refine 3D reconstruction results, 3D scenes generated from the Reconstruct were imported into 3D Studio Max for further smoothing and rendering. The final 3D rendering results are shown in [Fig. 6](#).

## 4. Discussion

### 4.1. Preparation and staining of serial sections

Several serial sectioning approaches can be applied for the dissection of tissue or organs. First, paraffin embedding allows

the easy production of serial sections that can be used for both HE and immunostaining. The quality of paraffin sections is better than that of cryosections. However, several aspects require special consideration with respect to 3D reconstruction: (a) formalin fixation may lead to the shrinkage of the tissue or organ, especially when the tissue has a high water content; (b) during the cutting procedure, the paraffin block may warm up, which will generate thicker sections in the next round of cutting; (c) some treatments with high temperature or organic solvent may affect the tissue morphology; (d) for immunostaining, antigen retrieval must be applied for many antigens.

Compared with paraffin sections, resin sections are a better alternative. Using this method, very thin sections can be cut and tissue morphology is very good, in most cases. However, this method also has some disadvantages. (a) If very thin sections are used, the multitude of sections generated will be difficult to handle. In our study, if sections of 2  $\mu\text{m}$  in thickness had been used, more than 1000 sections would have been produced; (b) resin embedding and resin sectioning is time consuming; (c) resin sections are not suitable for immunostaining.

In our study, snap frozen tissue blocks were cut on a cryostat for the preparation of the serial sections of the PP. By using a lower cutting temperature ( $-22$  to  $-24$  °C) and precise temperature control of the box and objective, we were able to produce serial sections of high quality. For the PP examined in our work, a total of 231 sections were produced and only 5 sections were discarded because of distortion. In the next step, the 10- $\mu\text{m}$ -thick serial sections were stained with our new HE staining protocol and good staining was obtained. Therefore, our sectioning and staining protocol were sufficient for our 3D reconstruction studies. Moreover, the use of cryosections avoided the need for antigen retrieval. When serial cryosectioning is combined with our new multiple colour staining method ([Ma et al., 2006](#)), up to six structures or cell populations with specific markers can be identified within the 3D environment of tissues or organs.

### 4.2. Stitching and registration of serial sections

Under bright-field or fluorescence microscopy, an analysis of a whole section of certain tissues or organs at high resolution sometimes cannot be performed, even at low power and even if cameras with high resolution are employed. For example, a whole image of the PP cannot be obtained with only one acquisition, even at 50 $\times$  magnification. Image “mosaicing” is a powerful approach for solving this problem by creating a single composite image by the overlapping of multiple images acquired from different parts of the section ([Süss et al., 2002](#)). The simplest way of mosaicing is to tile serial images one after another. However, even when a very precise motorized stage is used, exact and seamless mosaicing is still difficult to achieve with this method. Therefore, instead of using simple tiling, image stitching can be applied. In our study, multiple images with a certain overlap with adjacent images from a part of PP were acquired separately and stitched with Image Pro Plus. The overlap of two adjacent images, which is needed for the

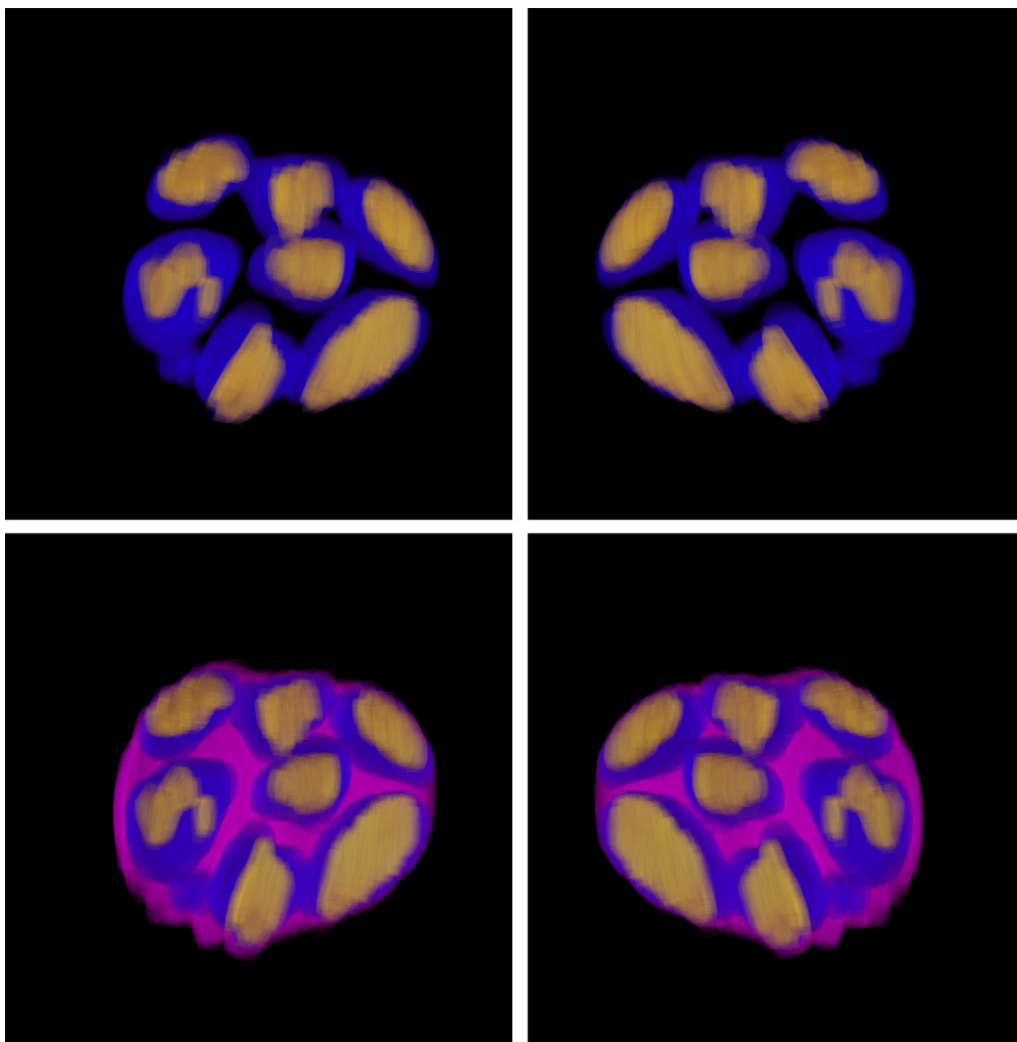


Fig. 5. 3D reconstruction of a mouse Peyer's patch by using Reconstruct. Two projections from the reconstructions results are shown. Section thickness: 2.0 pixels; yellow: germinal centre; blue: follicle; magenta: Peyer's patch. (Left) Front side is the intestine lumen. (Right) 180° rotation version of image on the left. Front side is the intestine serosa.

stitching, is dependent mainly on the accuracy of the motorized stage. For example, with some motorized stages with low accuracy, an overlap of up to 30% is needed for stitching. In our studies, a 12% overlap was set for the acquisition and good stitching results were obtained.

For the alignment of serial sections, both manual and automatic approaches can be used. In our study, a manual registration method instead of an automatic technique has been applied. The time needed for the alignment of 226 serial sections is only 16 h, which is acceptable for the reconstruction process. Normally, manual alignment is time consuming and multiple manipulations lead to the loss of image information. However, by using Reconstruct, the registration process is much faster and easier because of the following reasons. First, the movement of the objects are performed at various increments, which greatly reduce the registration time. Second, since the manipulation is not carried out on “real”, the loss of image information can be avoided. The third is that the blending of the two adjacent sections during registration, which means the real-time visualization of the registration results, can make the alignment

much easier and more precise. In addition, this method is a universal registration method. Even if the sections have artefacts such as distortions or severe uneven illumination, which may make the normal correlation-based registration method difficult to perform, good registration can be achieved.

#### 4.3. 3D reconstruction of PP

Three different kinds of approaches were applied for the 3D reconstruction of the PP.

First, Image J was used for the “real” high-resolution reconstruction of the PP. This method is an easy and efficient way for the reconstruction of PP at high resolution and for the generation of a virtual PP. This kind of virtual PP can be regarded as a database for the whole PP and may be re-sliced in any direction for further analysis. Since the distance between two adjacent sections is 2.13 pixels, interpolation was used to “fill” the interval between two sections.

Second, Reconstruct was applied for the reconstruction. To perform this kind of reconstruction, objects of interest should

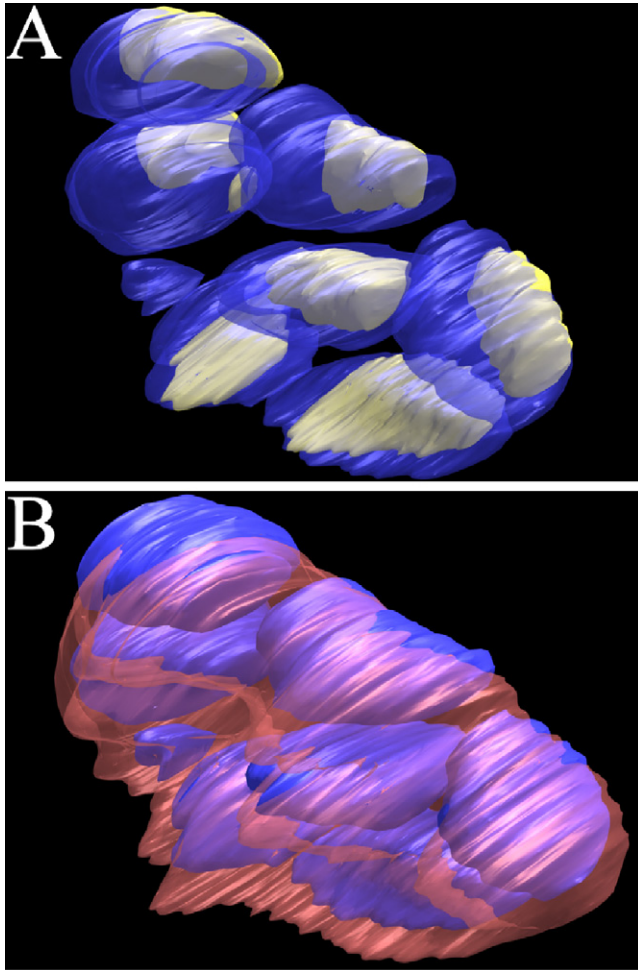


Fig. 6. 3D reconstruction of mouse Peyer's patch by using Reconstruct and 3D Studio Max. In Reconstruct, sets of objects were imported to the 3D scene and exported as VRML files. These VRML files were then imported to 3D Studio Max for smoothing and rendering. Yellow: germinal centre; blue: follicle; magenta: Peyer's patch. (A) B cell follicles and their associated germinal centres; (B) Peyer's patch and their B cell follicles.

be first segmented. In our study, the B cell follicle and germinal centre were segmented according to their morphology and correlation between adjacent sections. This type of segmentation, which is different from the segmentation in electron microscopic images, is time consuming. However, no program can distinguish the B cell follicle from other compartments automatically. However, by using immunostaining, some structures such as lymphatic vessels and blood vessels can be segmented according the colour properties of the images (Ma et al., 2006). This segmentation method is faster and more efficient than manual segmentation. In further studies, we intend to combine multiple colour immunolabelling and segmentation approaches in the 3D reconstruction of secondary lymphoid tissues or organs.

Third, 3D Studio Max was applied for the refinement of the reconstruction results of the PP. Although the smoothing undertaken will lead to the loss of information, it will improve the reconstruction results. The surface model generated from Reconstruct was imported to 3D Studio Max and new rendering

was performed after two steps of object smoothing. Similar approaches for the refinement of the reconstruction have been reported previously (Guest and Baldock, 1996). Normally, with these kinds of methods, the whole 3D model is a simplified one because of the simplification of the objects in the tissues or organs.

#### 4.4. 3D organization of the PP

Although many studies have been reported concerning the functional anatomy of PP, the precise 3D arrangement of B and T cells in the different compartments is largely unknown. In our study, the relative organization of the germinal centre, follicle and other compartments has been clearly revealed. According to our study, the PP studied contains eight follicles of different sizes. In most of the follicles, a germinal centre can be found, which is different from the lymph node in the case of the pathogen-free mouse. By using Reconstruct, the volume of some compartments, e.g. the germinal centres and the B cell follicle, could be measured. The volume of the germinal centre is about 11–36% of that of the follicle. This kind of stereological analysis will be helpful for the future quantitative analysis of PP anatomy during normal and abnormal immune responses. For example, it can be used for a similar comparative study of the dynamics of the germinal centre before and after an immune response (Hauser et al., 2007).

Using the 3D reconstruction methods described here, we intend to create better virtual PP models, which will be important for studies of immune cell dynamics and *in vivo* microscopy. This kind of virtual PP can now be resliced, “explored” and analysed by various morphological methods.

In summary, we have accomplished the 3D reconstruction of the PP by using serial sections. The combinational approaches that we present here should be useful for the reconstruction of various tissues or organs. In addition, the 3D model created by our methods and the stereological analysis should be helpful for further studies of the PP during the immune response.

#### Acknowledgements

We acknowledge the financial support from the University Hospital of Ulm, Germany. We also thank Dr. Wayne Rasband for the Image J program and Dr. John C. Fiala for the Reconstruct program.

#### Appendix A. Supplementary data

Supplementary data associated with this article can be found, in the online version, at [doi:10.1016/j.micron.2007.10.007](https://doi.org/10.1016/j.micron.2007.10.007).

#### References

- Bargatze, R.F., Jutila, M.A., Butcher, E.C., 1995. Distinct roles of L-selectin and integrins  $\alpha_4\beta_7$  and LFA-1 in lymphocyte homing to Peyer's patch-HEV in situ: the multistep model confirmed and refined. *Immunity* 3, 99–108.
- Brandtzaeg, P., Pabst, R., 2004. Let's go mucosal: communication on slippery ground. *Trends Immunol.* 25, 570–577.

- Ermak, T.H., Owen, R.L., 1986. Differential distribution of lymphocytes and accessory cells in mouse Peyer's patches. *Anat. Rec.* 215, 144–152.
- Fujimura, A., Nozaka, Y., 2002. Analysis of the three-dimensional lymphatic architecture of the periodontal tissue using a new 3D reconstruction method. *Microsc. Res. Tech.* 56, 60–65.
- Guest, E., Baldock, R., 1996. Automatic reconstruction of serial sections using the finite element method. *Bioimaging* 3, 154–167.
- Hauser, A.E., Junt, T., Mempel, T.R., Sneddon, M.W., Kleinstein, S.H., Henrickson, S.E., von Andrian, U.H., Shlomchik, M.J., Haberman, A.M., 2007. Definition of germinal-center B cell migration in vivo reveals predominant intrazonal circulation patterns. *Immunity* 26, 655–667.
- Iwasaki, A., 2007. Mucosal dendritic cells. *Annu. Rev. Immunol.* 25, 381–418.
- Ju, T., Warren, J., Carson, J., Bello, M., Kakadiaris, I., Chiu, W., Thaller, C., Eichele, G., 2006. 3D volume reconstruction of a mouse brain from histological sections using warp filtering. *J. Neurosci. Methods* 156, 84–100.
- Kelsall, B.L., Strober, W., 1996. Distinct populations of dendritic cells are present in the subepithelial dome and T cell regions of the murine Peyer's patch. *J. Exp. Med.* 183, 237–247.
- Kunkel, E.J., Ramos, C.L., Steeber, D.A., Muller, W., Wagner, N., Tedder, T.F., Ley, K., 1998. The roles of L-selectin, beta 7 integrins, and P-selectin in leukocyte rolling and adhesion in high endothelial venules of Peyer's patches. *J. Immunol.* 161, 2449–2456.
- Ma, B., Winkelbach, S., Lindenmaier, W., Dittmar, K.E., 2006. Six-colour fluorescent imaging of lymphoid tissue based on colour addition theory. *Acta Histochem.* 108, 243–257.
- Ma, B., von Wasielewski, R., Lindenmaier, W., Dittmar, K.E., 2007a. Immunohistochemical study of the blood and lymphatic vasculature and the innervation of mouse gut and gut-associated lymphoid tissue. *Anat. Histol. Embryol.* 36, 62–74.
- Ma, B., Zimmermann, T., Rohde, M., Winkelbach, S., He, F., Lindenmaier, W., Dittmar, K.E., 2007b. Use of Autostitch for automatic stitching of microscope images. *Micron* 38, 492–499.
- Ma, B., Lin, Z., Winkelbach, S., Lindenmaier, W., Dittmar, K.E. Automatic registration of serial sections of mouse lymph node by using Image-Reg. *Micron*, in press.
- Okada, T., Ngo, V.N., Ekland, E.H., Forster, R., Lipp, M., Littman, D.R., Cyster, J.G., 2002. Chemokine requirements for B cell entry to lymph nodes and Peyer's patches. *J. Exp. Med.* 196, 65–75.
- Sato, A., Iwasaki, A., 2005. Peyer's patch dendritic cells as regulators of mucosal adaptive immunity. *Cell Mol. Life Sci.* 62, 1333–1338.
- Steiniger, B., Ruttinger, L., Barth, P.J., 2003. The three-dimensional structure of human splenic white pulp compartments. *J. Histochem. Cytochem.* 51, 655–664.
- Steinman, R.M., Witmer, M.D., 1984. The anatomy of peripheral lymphoid organs with emphasis on accessory cells: light-microscopic immunocytochemical studies of mouse spleen, lymph node, and Peyer's patch. *Am. J. Anat.* 170, 465–481.
- Süss, M., Washausen, S., Kuhn, H.J., Knabe, W., 2002. High resolution scanning and three-dimensional reconstruction of cellular events in large objects during brain development. *J. Neurosci. Methods* 113, 147–158.
- Wagner, N., Lohler, J., Kunkel, E.J., Ley, K., Leung, E., Krissansen, G., Rajewsky, K., Muller, W., 1996. Critical role for beta7 integrins in formation of the gut-associated lymphoid tissue. *Nature* 382, 366–370.
- Warnock, R.A., Campbell, J.J., Dorf, M.E., Matsuzawa, A., McEvoy, L.M., Butcher, E.C., 2000. The role of chemokines in the microenvironmental control of T versus B cell arrest in Peyer's patch high endothelial venules. *J. Exp. Med.* 191, 77–88.
- Young, L.J., McFarlane, R., Slender, A.L., Deane, E.M., 2003. Histological and immunohistological investigation of the lymphoid tissue in normal and mycobacteria-affected specimens of the rufous hare-wallaby (*Lagorchestes hirsutus*). *J. Anat.* 202, 315–325.